Broad-Spectrum Electron Gun for Laboratory Simulation of Orbital Environments

Miles T. Bengtson *, Kieran T. Wilson† and Hanspeter Schaub‡
Aerospace Engineering Sciences Department, University of Colorado, Boulder, Colorado, 80303

A novel type of electron gun is discussed which emits electrons across a broad spectrum of energies. The motivation is to closely match the space environment with electron emission that is capable of a custom continuous range of energies and densities. Laboratory experiments to study spacecraft charging and space weathering are limited by the inability of conventional monoenergetic electron beams to produce space-representative electron fluxes. The new broad-spectrum electron gun enables straightforward and cost-effective simulation of the space electron flux environment in a laboratory vacuum chamber. A prototype device is used to create continuous spectra between 1 eV and 9 keV, with tests in progress to demonstrate continuous spectra up to 30 keV and higher. A future prototype is discussed which allows for arbitrary tuning of the output spectra to closely match a desired space environment. This device represents a significant advancement for the experimental spacecraft charging and space weathering communities by allowing test samples to be studied in the same electron flux environment in which they operate.

I. Introduction

Materials on the exterior of spacecraft are directly exposed to the extreme space environment which contains fluxes of high energy electrons. When charged particles impact a surface, they deposit both energy and charge, degrading the optical, mechanical, and electrical properties of the material [1–3]. As a result, spacecraft can charge to large potentials and experience electrostatic discharges between differentially charged surfaces. The discharges or arcs can lead to spacecraft anomalies, which are difficult to resolve, or even premature mission loss [4]. The differential charging behavior of a space object is directly dependent on the instantaneous state of its materials at a given point during its mission lifetime. Therefore, it is critically important to understand the interactions between the environment and spacecraft materials to ensure safe, long-term operation of assets on-orbit.

Laboratory tests are frequently conducted in which materials are exposed to energetic electron beams to study on-orbit spacecraft charging and material degradation (e.g. [1, 5–7]). One particular challenge in simulating the space environment is in generating realistic electron energy distributions. Conventional electron guns only emit at a single energy, whereas the space environment consists of electrons across a broad-spectrum of energies. It is widely known that the material degradation and charging/discharging characteristics depend on the energy of the incident electrons [8–10]. Furthermore, it has been established that exposing a material to a combination of two or three beams with different energies produces different charging/discharging behavior than exposing it to a single, monoenergetic beam [11, 12]. For example, high-energy particles may pass through a dielectric material without depositing any charge, but may modify the electrical properties of the material through radiation-induced conductivity [3]. Low-energy particles do not pass through the material and thus deposit charge into the surface. The point at which the dielectric breaks down and experience discharge depends on the fluxes of particles at different energies. Therefore, it is critically important to consider the full spectrum of incident electrons to accurately reproduce the charging and breakdown behavior of dielectrics exposed to space radiation.

Reference [13] shows that materials exposed to low energy (<1 keV) electrons, which have sometimes been neglected in orbital flux and energy deposition models in the past, exhibit optical changes which are a significant fraction of changes induced by orbital or higher energy exposures. Therefore, it is questionable how well tests using monoenergetic beams actually represent on-orbit behavior. It is therefore highly desirable to be able to expose materials to a broad spectrum of electron energies in the laboratory.

*Graduate Research Assistant, Aerospace Engineering Sciences, 3775 Discovery Drive, Boulder, CO 80303, AIAA Member
†Graduate Research Assistant, Aerospace Engineering Sciences, 3775 Discovery Drive, Boulder, CO 80303, AIAA Member
‡Professor, Glenn L. Murphy Endowed Chair, Aerospace Engineering Sciences, 3775 Discovery Drive, Boulder, CO 80303, AIAA and AAS Fellow

Currently, there is not a straightforward and experimentally-tractable means to generate a broad-spectrum electron flux environment in the eV to 100 keV range in the laboratory. Reference [14] presents a concept for generating broad-spectrum fluxes in which a high energy monoenergetic beam is passed through a series of thin foils. The monoenergetic beam experiences energy scattering as it interacts with the thin foils, thereby creating a spectrum of energies. Preliminary experiments with this device in the 1980s showed significant differences in the charging/discharging characteristics of Kapton when exposed to the spectral versus monoenergetic electron flux environments [15, 16].

To the best of our knowledge, only one facility is in operation today which produces spectral beams by passing a monoenergetic beam created via a high-power accelerator through a scattering foil [17]. However, this facility requires the use of a Van de Graaff accelerator to generate the initial 400 keV beam, making this technique prohibitively expensive to be widely useful. In addition, this facility models the higher energy (hundreds of keV) portion of the spectrum well, but requires a monoenergetic beam in the tens of keV range to complete the spectrum at lower energies [18, 19]. Strontium-90 has also been identified as a potential source of spectral electron fluxes [11, 20]. However, the β-decay from Sr-90 is also in the hundreds of keV to MeV range, and thus does not address the need for spectral fluxes in the tens of keV range.

Currently, the best practice for recreating on-orbit damage in the laboratory is to expose test samples to a sequence of monoenergetic electron beams which approximate the dose-depth curve experienced on-orbit [21, 22]. However, this process requires tests at numerous energies to accurately model the on-orbit environment, which is both costly and time-consuming. Further, it is known that materials experience recovery post-irradiation, even if they are kept in vacuum, so there may be competing processes of recovery and degradation during the time required to expose the sample to many different beams [10]. Therefore, there is a clear need for a broad energy spectrum electron source which can accurately reproduce the electron spectra observed on-orbit.

This paper presents a concept for a broad-spectrum electron gun which enables accurate laboratory simulation of on-orbit energetic electron fluxes. The novel source presented herein provides a cost-effective, robust, and experimentally-tractable means to generate spectral fluxes in the eV to tens of keV range. The remainder of the paper is organized as follows. Section II describes the theory and concept of the electron gun, and Section III provides results from a prototype model which demonstrate the ability of the device to generate broadband energetic electron spectra. This electron gun design enables future experiments which will be critically important for understanding, modeling, and predicting spacecraft charging and material degradation.

II. Theory and Design

A. Principle of Operation

Figure 1 shows a schematic of the electron gun design. Ultraviolet light is used to stimulate photoelectron emission from inside a hollow tube, which consists of a series of n individual circular stages. The stages are each held at different potentials and are stacked together with thin insulators in between each stage for electrical isolation. The circular shape of each ring acts like an Einzel lens to focus the electrons toward the center of the device and into a beam. Each stage being held at a different potential sets up an electric field along the length of the device that accelerates the electrons toward the aperture. The forward most stage is at zero potential, which contains the electric fields within the device. The rearward most stage has a grid placed over the aperture which allows the UV light to shine in while also containing the electric fields. Each electron is generated on a stage at a given negative voltage, then accelerated toward the front of the device which is grounded. Therefore, the final energy of each electron is equal to the (negative) voltage of the stage on which it was generated. This design enables the device to emit an electron beam with a total number of energies equal to the number of stages.

In theory, the maximum energy electron capable of being produced by the broad-spectrum source is limited only by the maximum voltage which a power supply can provide. Commercially-available power supplies are available which output voltages up to the hundreds of kV range. Linacs, cyclotrons or other types of accelerators that do not rely on static electric fields to accelerate charged particles are generally required to generate particle fluxes in the MeV range [23]. Therefore, it is expected that the broad-spectrum gun design would be capable of producing electrons in the range from eV to hundreds of keV. This range is highly relevant for spacecraft surface charging, material degradation, and instrument calibration purposes.

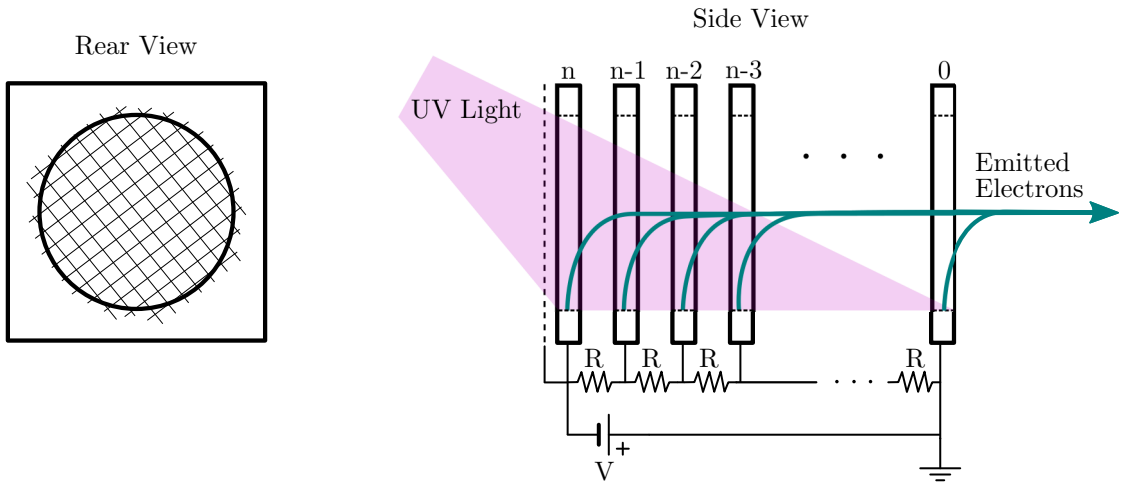

Fig. 1 Schematic of the broad-spectrum electron gun design and operation. The side view shows how the voltage gradient is applied to the stages and how the UV light is used to stimulate photoelectron emission from each stage. The rear view shows the shape of each stage with a grid (on the rearmost stage only) to contain the electric fields.

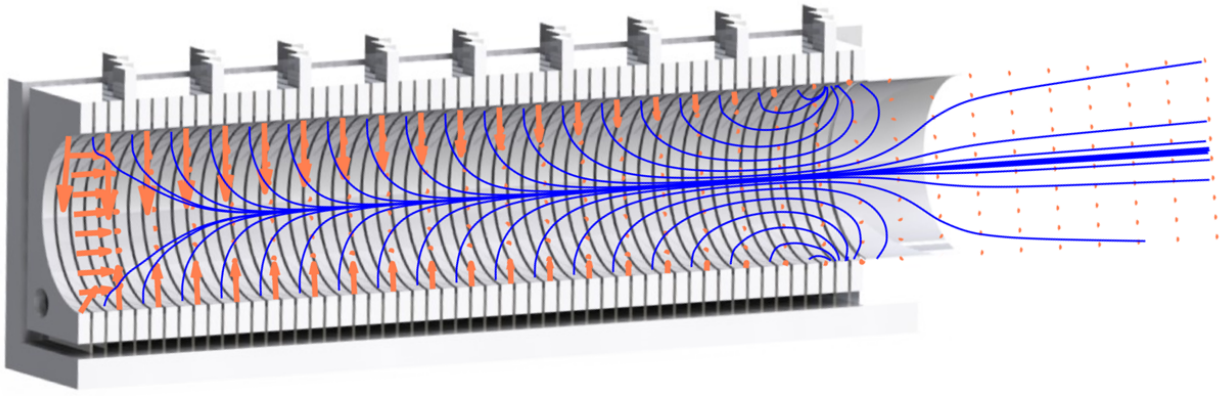

Fig. 2 Electric field streamlines (blue) and electric field (orange arrows) imposed on the electron gun CAD model with 54 discrete stages.

B. Device Prototype

A prototype has been constructed which consists of 54 aluminum stages with thin Delrin insulators in between each stage, yielding a near-continuous approximation of a spectrum. A CAD model of the broad-spectrum source is shown in Figure 2, with orange arrows indicating electric field vectors and blue lines indicating electric field streamlines. Pictures of the device are shown in Figure 3 and 4. 10 MΩ space-rated resistors are used in the voltage divider circuit. The large resistances were selected to keep the current draw from the power supplies low. A Hamamatsu L10706 vacuum ultraviolet light (not pictured) is used to stimulate photoemission inside the tube. This source emits across a distribution from 115 to 400 nm, with a primary peak at 161 nm (equivalent to 7.70 eV) [24].

An interesting trade space exists related to the number of stages used in a given design. First, the broad-spectrum gun outputs a quasi-continuous spectrum, and using more stages leads to a better approximation of a fully-continuous spectrum. Using more stages also reduces the voltage step in between each stage, therefore reducing the likelihood of arcing between stages. For example, if a maximum voltage of 30 kV is applied to the rearmost stage and only 10 stages are used, there is a 3 kV potential difference between adjacent stages (assuming all resistors are sized equally). However, if 100 stages are used, the potential difference between stages is only 300 V, which significantly reduces the risk of arcing between stages. The downside to adding more stages is that it increases the physical size of the device and adds complexity (though compared to many scientific sources and detectors, the broad-spectrum electron gun is still a

relatively straightforward device). The 54 stage prototype is approximately 33 cm long with a 6×6 cm cross section. In its current form, the entire device must fit inside the vacuum chamber. Future iterations will be flange-mountable so that the gun can be installed on the outside of a vacuum chamber.

III. Results and Discussion

A. Initial Testing

The broad-spectrum electron gun prototype was tested in a vacuum chamber with a variety of maximum voltages, ranging from 500 V to 9 kV. A computer-controllable Matsusada AU series high-voltage power supply was used to apply voltage to the electron gun. A custom-built retarding potential analyzer (RPA) was used to measure the electron fluxes output by the electron gun. This particular RPA has been described extensively in other publications [25, 26]. The RPA was mounted on an in-vacuum linear motion stage to allow for characterization of the beam. Tests were conducted with vacuum chamber pressures on the order of 10^{-5} torr. One significant advantage of the broad spectrum source is that it does not rely on fragile filaments which are common in conventional electron guns. As a result, the broad-spectrum source is more rugged and does not have as stringent cleanliness and vacuum requirements as filament-based guns.

Figure 5 compares electron gun output fluxes to electron fluxes at geosynchronous orbit (GEO) as measured by the Los Alamos National Lab Magnetospheric Plasma Analyzer instruments [27]. Ideally, the maximum energy limit is determined only by the maximum output of available power supplies, and the maximum energy is easily tunable. In practice, however, the electron gun experiences arcing when voltages greater than 9 kV are applied to the rearmost stage. Work is ongoing to identify likely arcing sites and improve the design so that operation at tens of kV can be achieved. Tests are currently underway to demonstrate electron gun performance for a spectrum up to 30 keV and future tests are planned up to 100 keV.

As shown in the figure, the electron gun outputs fluxes which are on the order of 10^{11} electrons/cm^2·s, whereas the fluxes encountered at GEO are on the order of 10^8 electrons/cm^2·s. The equivalent fluence from one year on orbit in GEO can be achieved in approximately 9 hours in the laboratory with the broad-spectrum source. Therefore, the source is appropriate for accelerated laboratory testing of on-orbit material degradation. The current design, however, uses a single, constant-intensity light source to stimulate photoemission from all of the stages, so no control over the output flux level is possible. It would be desirable for many tests to output fluxes which are representative of the actual GEO environment, rather than tuned for accelerated lifecycle testing. Future iterations should incorporate sources with controllable intensities so the output fluxes can be adjusted as required for a given experiment.

An additional effect of the current design only using a single light source is that there is an uneven distribution of VUV light falling on the interior of the device. This causes more or fewer electrons to be generated at a given energy depending on the amount of light which falls on a given stage. Figure 6 shows an example differential flux spectrum for when the maximum voltage applied to the gun is 950 V. Due to the alignment between the VUV light source and the gun, most of the light falls on the rear stages, which is why there is a peak at 900 eV. The fluxes are lower in the 300-600 eV range, then there is a peak again at approximately 100 eV. This peak is caused by higher energy electrons from the rear stages impacting the front stages and generating secondary electrons from these stages.

B. Spatial-Energy Distribution

A beam map was collected to determine the spatial flux and current distribution output from the gun. The RPA was mounted vertically on the motion system and the broad-spectrum gun was mounted above it. The RPA was swept across the beam and a spectrum like that shown in Figure 6 was collected at each position. Figure 7 shows a series of photographs of the RPA inside the chamber during the data collection and being swept beneath the electron gun aperture.

Figure 8 shows a 1D beam map taken when the electron gun was set to output a maximum energy of 500 eV. Figure 9 shows a beam map for a maximum output energy of 950 eV. Overall, both plots show a beam spot size on the order of 3-4 cm, though there is some energy-dependent focusing and spreading. Several interesting features are visible in the data. First, hot spots are present in both plots at approximately 90% of the maximum energy. The peak in the 500 eV spectrum is larger than that in the 950 eV. Medium energy electrons are deflected by 1-2 cm, so distributions are not centered about the zero position. Again, this is a consequence of only using a single light source which is directed at one side of the electron gun. This causes electrons to be emitted from the gun at an angle which depends on the electron energy.

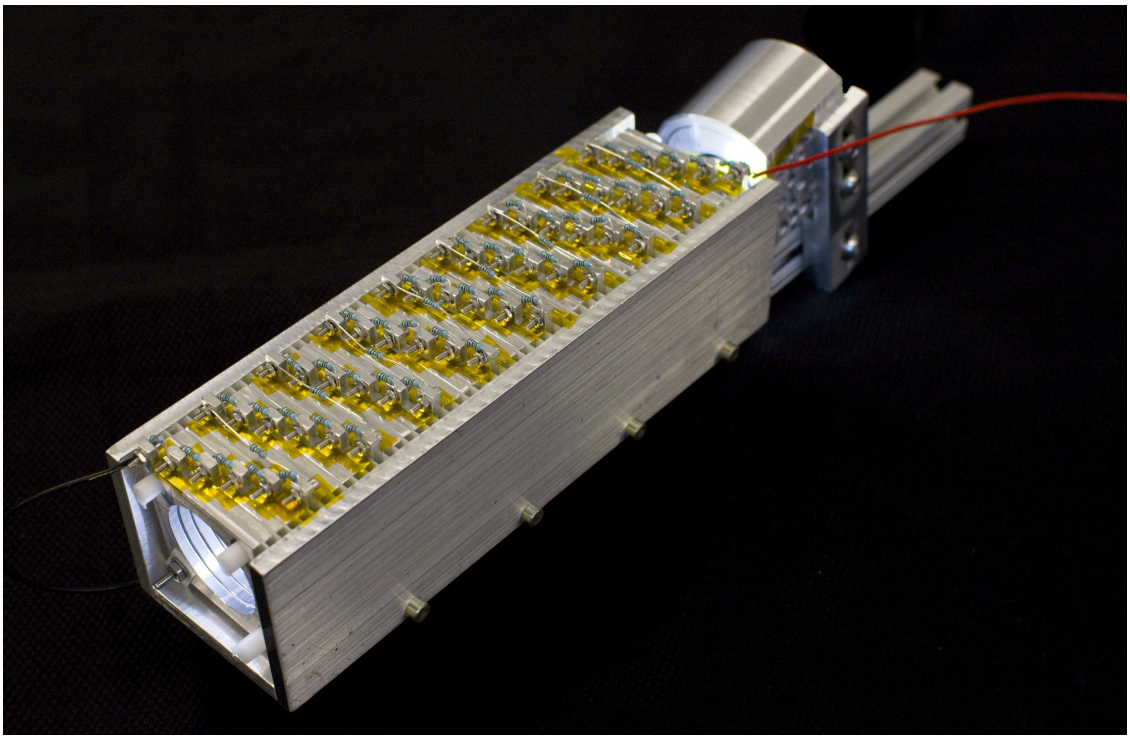

Fig. 3 Prototype of the broad-spectrum electron gun with 54 discrete stages.

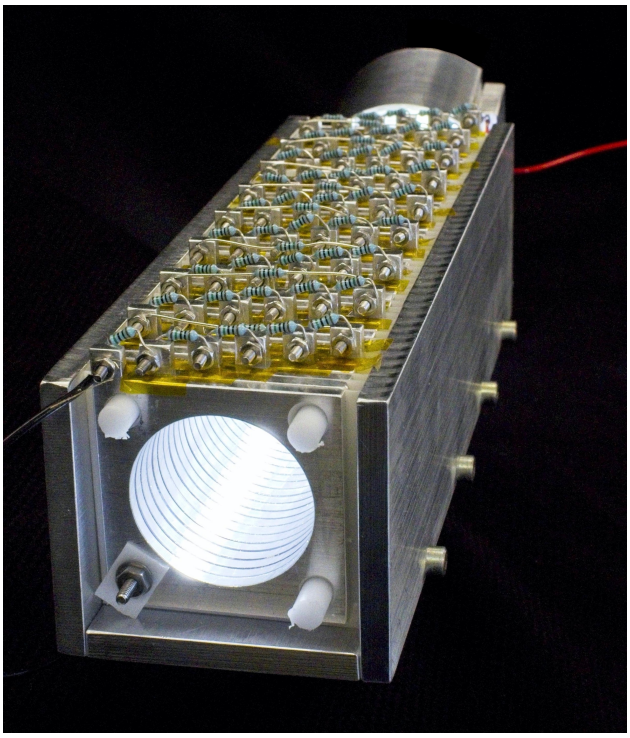

Fig. 4 Front view of the broad-spectrum electron gun.

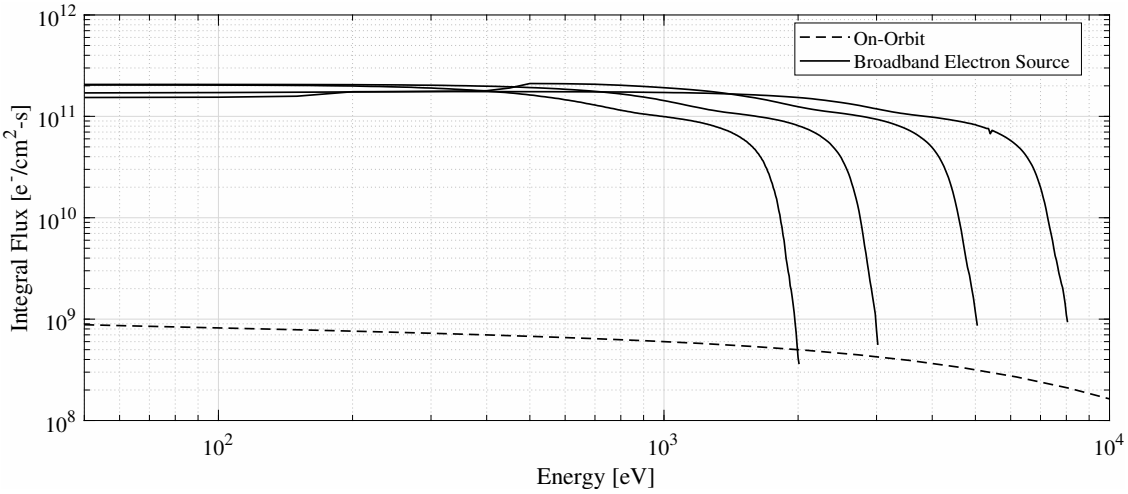

Fig. 5 Example output spectrum from the broad-spectrum electron gun up to 8 keV compared to data from GEO [27].

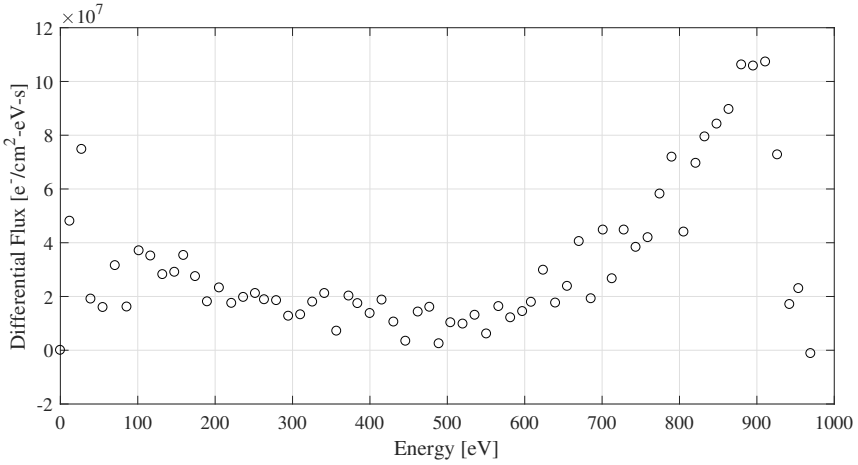

Fig. 6 Differential electron flux spectrum taken with a maximum energy of 950 eV applied to the gun and the RPA located at the gun exit plane.

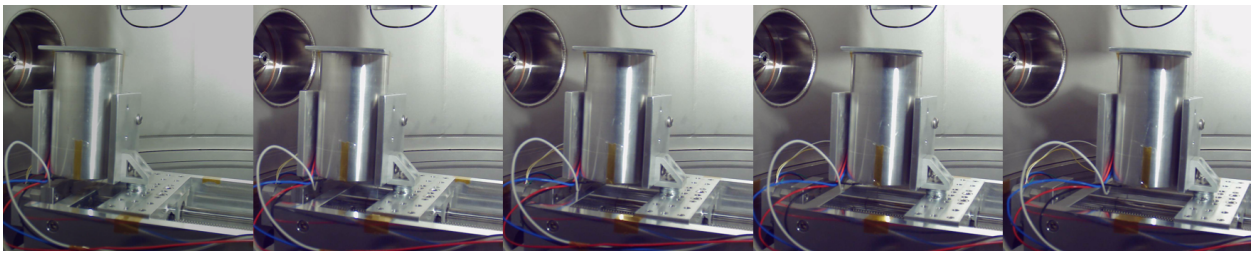

Fig. 7 Series of photographs showing the RPA mounted on the linear translation stage inside the vacuum chamber. The RPA is translated beneath the aperture of the broad-spectrum source to measure the spatial distribution of the electron beam. The aperture of the electron source is visible at the top of each photograph.

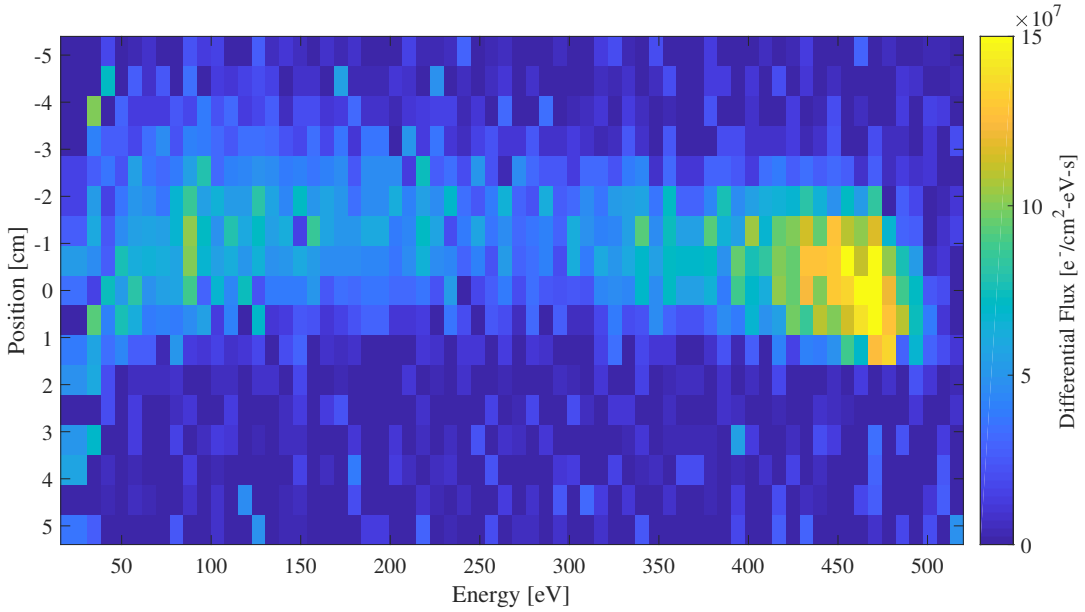

Fig. 8 Beam map for maximum energy of 500 eV.

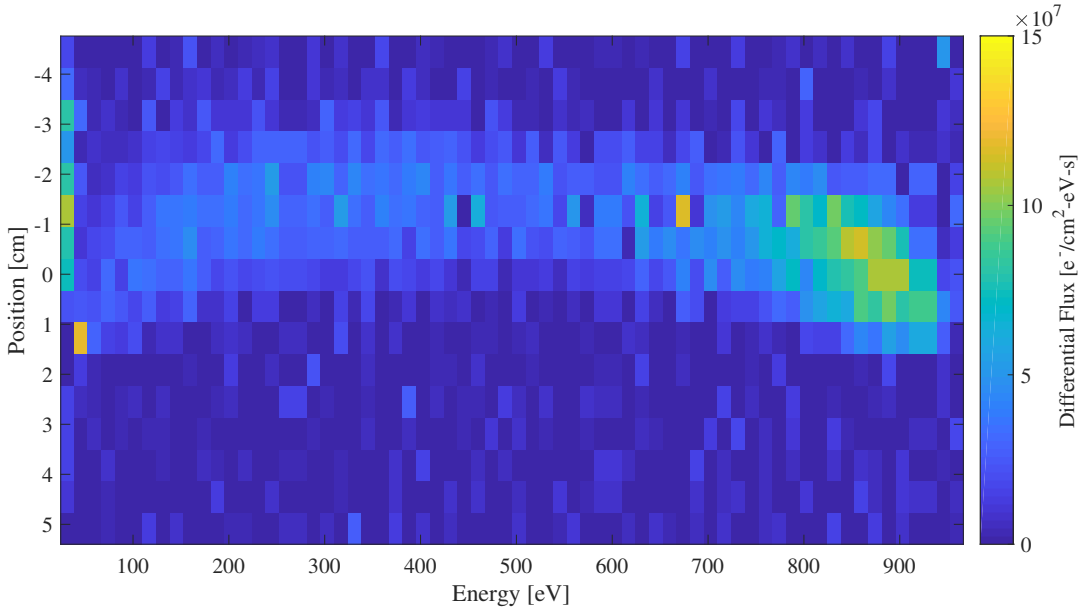

Fig. 9 Beam map for maximum energy of 950 eV.

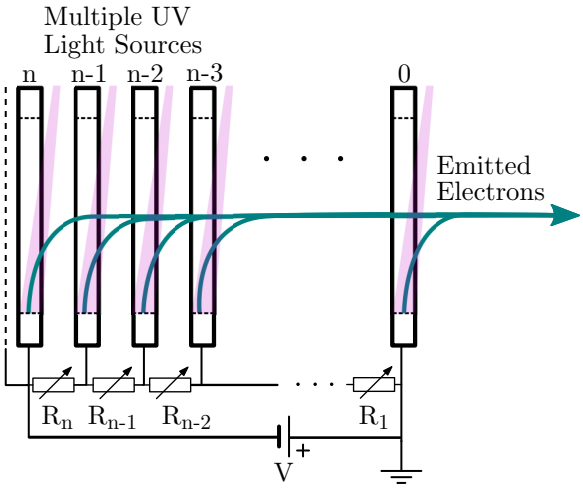

Fig. 10 Possible future improvements to the broad-spectrum electron gun.

IV. Future Improvements

Several future improvements are possible which will enable the broad-spectrum source to better serve the needs of the spacecraft charging community. The existing prototype uses only a single light source which outputs at a constant intensity. As a result, the shape of the output spectrum is fixed. Future iterations may incorporate multiple light sources along the axis of the electron gun. By adjusting the intensity of each of these sources, the number of electrons produced at a given energy can be varied and the resultant spectrum can be tuned arbitrarily. One challenge here is that the light source currently in use outputs at 161 nm (7.70 eV), whereas smaller light sources, such as UV diodes which are small, dimmable, and cost-effective, are limited to wavelengths in the 250 nm (4.96 eV) and above range. Though aluminum has a work function of 4.08 eV [28], the formation of oxide layers on the aluminum surface increases the work function to approximately 6 eV [29]. As a result, the light from the diode sources is not sufficiently energetic to excite photoemission from the surface. To solve this problem, either light sources with shorter wavelengths must be used to exite photoelectrons in spite of the oxide layers or the emitting surfaces must be treated to lower the work function. The aluminum surfaces could be atomically cleaned to remove the oxide layers (necessitating that they be kept in vacuum in between cleaning and use), or treated with a low work function coating. Work is ongoing to determine the best solution within this trade space.

Another advantage to using multiple light sources is the ability to achieve even light distribution on the inside of the hollow tube. In the current configuration, the light only falls on one side of hollow tube, and the beam spot is non-uniform (hence the crescent shape in Figures 8 and 9). Distributing the light sources such that the light distribution is uniform would help create a circular beam spot with uniform energy distribution. Another consideration is that some applications may require a larger beam spot than the approximately 3 cm beam achieved with the existing prototype. Future studies should consider the effect of scaling the hollow tube diameter on the energy distribution of the beam. It would also be possible to stack several individual sources into an array to create a large beam spot size.

The implementation of multiple, adjustable-intensity light sources is one mechanism by which the output spectrum can be tuned arbitrarily. An additional mechanism is varying the voltage gradient applied to the device. The resistors in between stages could be replaced with digital potentiometers to allow for arbitrary adjustment of the voltage gradient applied to the device. Future tests will consider both of these techniques to determine how best to achieve full control over the output spectrum.

Finally, there is risk of charge deposition into the insulating Delrin sheets within the current design. Buildup of charge over extended periods of operation could affect the electric fields within the device and adversely affect the quality of the output fluxes. To mitigate this issue, the insulating Delrin sheets are to be replaced with small ruby or sapphire precision spheres. The spheres will fit into divots in each stage, providing consistent mechanical separation and electric insulation between stages while minimizing the presence of dielectrics within the device.

V. Conclusion

A new type of broad-spectrum electron gun has designed and developed. A prototype has been used to demonstrate the output of continuous spectra from 1 eV up to 9 keV with fluxes that are relevant for simulating a GEO environment. Work is ongoing to create spectra from 1 eV up to 100 keV and to allow for arbitrary adjustment of the spectra. Several avenues for future improvement of the device have been identified with the goal of creating a fully tunable spectrum of electron fluxes over 5 orders of magnitude in energy. The novel broad-spectrum electron gun is a capability that allows for significantly improved accuracy in laboratory studies of spacecraft-space environment interactions. Efforts are underway to make this device available to the experimental space weather communities.

Acknowledgments

The authors thank Dalton Turpen for assistance with design, manufacture, and testing of the broad-spectrum electron gun. Additionally, the authors thank Ryan Hoffmann and Dan Engelhart for technical advice and fruitful discussions on the topic and Joshua Bennett for managing and securing the intellectual property. M.T. Bengtson gratefully acknowledges funding from the NDSEG Fellowship.

References

[1] Tonon, C., Duvignacq, C., Teyssee, G., and Dinguirard, M., "Degradation of the optical properties of ZnO-based thermal control coatings in simulated space environment," *Journal of Physics D: Applied Physics*, Vol. 34, No. 1, 2001, p. 124.

[2] Plis, E. A., Engelhart, D. P., Cooper, R., Johnston, W. R., Ferguson, D., and Hoffmann, R., "Review of Radiation-Induced Effects in Polyimide," *Applied Sciences*, Vol. 9, No. 10, 2019, p. 1999.

[3] Paulmier, T., Dirassen, B., Arnaout, M., Payan, D., and Balcon, N., "Radiation-induced conductivity of space used polymers under high energy electron irradiation," *IEEE Transactions on Plasma Science*, Vol. 43, No. 9, 2015, pp. 2907–2914.

[4] Ferguson, D., White, S., Rast, R., and Holeman, E., "The Case for Global Positioning System Arcing and High Satellite Arc Rates," *IEEE Transactions on Plasma Science*, Vol. 47, No. 8, 2019, pp. 3834–3841.

[5] Feng, W., Ding, Y., Yan, D., Liu, X., Wang, W., and Li, D., "Combined Low-Energy Environment Stimulation Test of Geosynchronous Satellite Thermal Control Coatings," *Journal of spacecraft and rockets*, Vol. 46, No. 1, 2009, pp. 11–14.

[6] Grossman, E., and Gouzman, I., "Space environment effects on polymers in low earth orbit," *Nuclear Instruments and Methods in Physics Research Section B: Beam Interactions with Materials and Atoms*, Vol. 208, 2003, pp. 48–57.

[7] Stuckey, W., and Meshishnek, M., "Space environmental stability of Tedlar with multi-layer coatings: space simulation testing results," Tech. rep., Aerospace Corporation, 2000.

[8] Li, C., Yang, D., He, S., and Mikhailov, M., "Effect of electron exposure on optical properties of aluminized polyimide film," *Journal of materials research*, Vol. 17, No. 9, 2002, pp. 2442–2446.

[9] Wang, X., He, S., and Yang, D., "Low-energy electron exposure effects on the optical properties of ZnO/K2 SiO3 thermal control coating," *Journal of materials research*, Vol. 17, No. 7, 2002, pp. 1766–1771.

[10] Fogdall, L. B., Cannaday, S. S., and Brown, R. R., "Electron Energy Dependence for In-Vacuum Degradation and Recovery in Thermal Control Surfaces," *Thermophysics: applications to thermal design of spacecraft*, Elsevier, 1970, pp. 219–248.

[11] Balmain, K., and Hirt, W., "Dielectric Surface Discharges: Effects of Combined Low-Energy and High-Energy Incident Electrons," *IEEE Transactions on Electrical Insulation*, , No. 5, 1983, pp. 498–503.

[12] Zhaoming, Y., Yanping, Z., and Reihong, G., "Charging and discharging of dielectric films irradiated by high-/medium-/low-energy electrons," *Acta Astronautica*, Vol. 15, No. 11, 1987, pp. 865–870.

[13] Ciofalo, M. R., Brady, M. E., Panetta, C. J., and Meshishnek, M. J., "Low-energy electron exposure of space materials," *Journal of Spacecraft and Rockets*, Vol. 48, No. 6, 2011, pp. 931–941.

[14] Adamo, R., and Nanevicz, J., "Development of a continuous broad-energy-spectrum electron source," 1983.

[15] Adamo, R., and Nanevicz, J., "Preliminary comparison of material charging properties using single-energy and multienergy electron beams," 1980.

[16] Coakley, P., Wild, N., and Treadaway, M., "Laboratory investigation of dielectric materials exposed to spectral electron environments (1 to 100 keV)," *IEEE Transactions on Nuclear Science*, Vol. 30, No. 6, 1983, pp. 4605–4609.

[17] Paulmier, T., Dirassen, B., Belhaj, M., Inguimbert, V., Payan, D., and Balcon, N., "Experimental test facilities for representative characterization of space used materials," 2014.

[18] Payan, D., Inguimbert, V., Mateo-Velez, J.-C., Sarrail, D., Paulmier, T., Roussel, J.-F., Dirassen, B., Boulay, F., and Girard, L., "ESD Related R&D Studies at CNES and ONERA," *Image*, Vol. 330, No. 540, 2008, p. 800.

[19] Dirassen, B., Levy, L., Reulet, R., and Payan, D., "The SIRENE facility-an improved method for simulating the charge of dielectrics in a charging electron environment," *Materials in a Space Environment*, Vol. 540, 2003, pp. 351–358.

[20] Dennison, J., Hartley, K., Montierth Phillipps, L., Dekany, J., Dyer, J. S., and Johnson, R. H., "Small Satellite Space Environments Effects Test Facility," 2014.

[21] ISO 15856:2010, "Space Systems – Space Environment – Simulation guidelines for radiation exposure of non-metallic materials," Standard, International Organization for Standardization, Geneva, CH, 8 2010.

[22] Ciofalo, M., Meshishnek, M., and Hennesy, A., "Space Environmental Effects Exposure Testing of Space Materials," *Applied Space Environments Conference*, 2019.

[23] Wangler, T. P., *RF Linear accelerators*, John Wiley & Sons, 2008.

[24] *S2D2 VUV Light Source Unit L10706 Series*, Hamamatsu, 3 2014.

[25] Bengtson, M., Wilson, K., and Schaub, H., "Experimental Results of Electron Method for Remote Spacecraft Charge Sensing," *Space Weather*, 2020.

[26] Bengtson, M., "Electron Method for Touchless Electrostatic Potential Sensing of Neighboring Spacecraft," Ph.D. thesis, University of Colorado Boulder, 12 2020.

[27] Thomsen, M., Denton, M., Lavraud, B., and Bodeau, M., "Statistics of plasma fluxes at geosynchronous orbit over more than a full solar cycle," *Space Weather*, Vol. 5, No. 3, 2007.

[28] Ashcroft, N. W., Mermin, N. D., et al., "Solid state physics," , 1976.

[29] Grard, R., and Tunaley, J., "Photoelectron sheath near a planar probe in interplanetary space," *Journal of Geophysical Research*, Vol. 76, No. 10, 1971, pp. 2498–2505.